MICROMECHANICAL YIELDING AND FAILURE OF CF/EPOXY UD- AND CROSS-PLY LAMINATES UNDER THERMAL AND MECHANICAL LOADING

Thomas Hobbiebrunken[1], Bodo Fiedler[2], Masaki Hojo[1], Mototsugu Tanaka[1], Shojiro Ochiai[3] and Karl Schulte[2]

[1] Department of Mechanical Engineering, Graduate School of Engineering, Kyoto University, Sakyo-ku, Kyoto 606-8501, Japan
[2]Polymer Composite Section, Technical University Hamburg-Harburg, Nesspriel 5, 21129 Hamburg, Germany
[3]International Innovation Center, Kyoto University, Sakyo-ku, Kyoto 606-8501, Japan

ABSTRACT

The deformation, yield and failure behaviour of a modified epoxy resin has been studied by thermomechanical experiments. Based on the experimental results the mechanical behaviour and the yield and failure criteria where established. A micromechanical finite element analysis (FEA) was carried out to investigate the formation of microscopic stresses in CF/epoxy composites during cooling from manufacturing temperature and mechanical loading. It was found that thermal residual stresses give a large contribution to transverse failure in thermosetting composites. Especially in cross-ply laminates, the microscopic residual stresses are large and highly tri-axial that failure can occur already during cooling.

1. INTRODUCTION

The strain to failure of unidirectional composites under transverse load is usually lower than in the unreinforced matrix material [1]. The reasons for this phenomenon can be understood considering the microstructure of a composite. Owing to the mismatch in coefficient of thermal expansion (CTE), residual stresses are generated in composites, which are cured at higher temperatures. For polymer matrix composites, the fibre has usually lower CTEs than the matrix. The resulting stresses after cooling are mainly tensile in the matrix and compressive in the fibre [2]. Furthermore, an applied load causes stress and strain magnifications in the matrix owing to the different mechanical properties of the constituents [3]. Even for a simple uni-directional load, the stress state is highly tri-axial. Studies of the failure initiation process in polymer matrix composites under consideration of residual stresses require detailed investigation of the matrix properties because the matrix properties are very sensitive to the temperature. Young's modulus, yield stresses, and CTEs vary over a wide range during cooling from manufacturing temperature to room temperature (RT). The temperature dependent non-linear matrix behaviour is one of the most important among them because matrix plasticity can reduce the microscopic stress state depending on the stress state. Since the yield stress increases with decreasing temperature, the formation of residual stresses and reduction by matrix yielding is a competing process [4].

In our previous studies, we showed the influence of the variation of the local fibre volume fraction on the initiation of transverse failure in a UD-laminate with thermosetting matrix [5]. Depending on the local fibre volume fraction, the residual stresses can improve or reduce the local composite transverse strength.

In the present work, we consider additional residual stresses caused by macroscopic constraints in a cross-ply laminate. In the first two sections the results of the thermomechanical experiments on the epoxy resin and the established yield and failure criteria are shown. In section 3, we explain the numerical procedure. In the last section, the numerical results of microscopic yield and failure analysis are shown. Finally, we summarize this paper.

2. MATERIALS

The unidirectional composite investigated in this work consists of a commercial epoxy system and carbon fibres (Toho Rayon HTA 6K) with a fibre volume fraction of V_f=60%.

The matrix systems are RTM6, an unmodified epoxy resin for RTM process, and 6376 a modified epoxy resin for prepreg system. Both resins are supplied by Hexel corp. The curing process was two hours at T_c=180°C followed by a post curing cycle for four hours at T_{pc}=190°C.

3. EXPERIMENTS

The investigation of initial failure under consideration of residual stresses requires a detailed research of the temperature dependent mechanical and thermal behaviour of the epoxy matrix. We carried out tension and torsion tests, dynamic mechanical thermal analysis (DMTA) and thermal mechanical analysis (TMA) on 6376. The testing procedure is described in our former paper [6] where the experimental results for RTM6 were also shown.

3.1 Tensile tests

Representative stress/strain-curves for the tensile experiments of 6376 at different temperatures are shown in Fig. 1. The stress/strain behaviour depends strongly on the temperature. As expected it becomes more non-linear and shows more ductility with increasing the temperature. Young's modulus, yield and fracture stress decrease and strain to failure increases. The Young's modulus at room temperature was measured from 5 tests as 3.7 GPa.

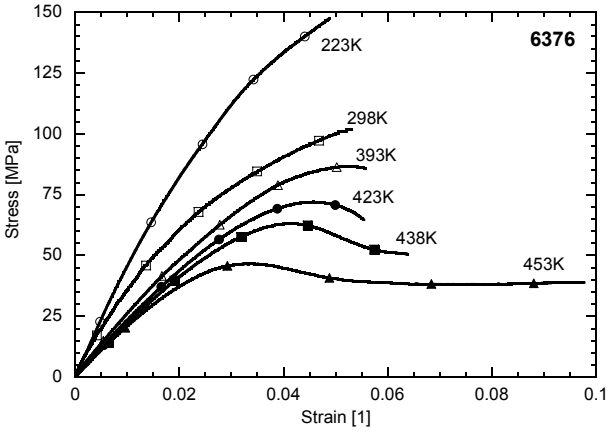

Fig. 1. Stress/Strain behaviour of 6376 at different temperatures.

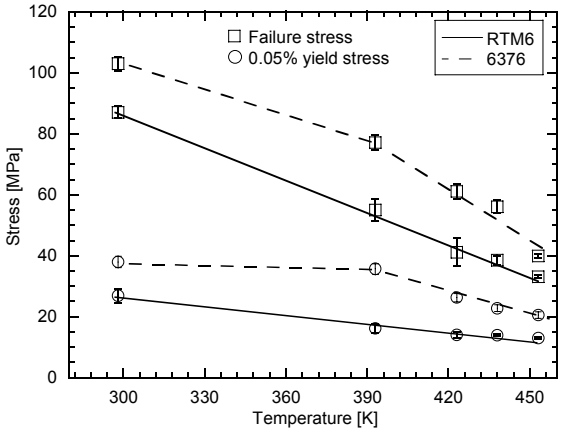

Fig. 2. Yield and failure stress of RTM6 and 6376 at different temperatures.

The yield and failure stresses are summarized in Fig 2. For comparison, the results of RTM6 are also shown. In the case of RTM6, a linear temperature dependency was found for the $\sigma_{0.05}$ and σ_f. Yield and fracture stress decrease from $\sigma_{0.05}$=26.8 MPa (σ_f=87.5 MPa) at 25°C to $\sigma_{0.05}$=13 MPa (σ_f=39.2 MPa) at 180°C. In the case of 6376 the temperature dependency can be assumed to be linear with a knee around 120°C (393K). For 6376 yield and fracture stresses are $\sigma_{0.05}$=37.9 MPa (σ_f =102.9 MPa) at 25°C and $\sigma_{0.05}$=20.5 MPa (σ_f =39.9 MPa) at 180°C and, thus these values are higher than for RTM6 for all temperatures.

3.2 Torsion tests

The stress/strain behaviour obtained from the torsion test is shown in Fig. 3. From the origin, the stress/strain behavior is linear elastic. With increasing strain, the resin shear behavior becomes non-linear and fails after reaching the maximum shear stress of σ_f=76.1±3.2 MPa. The final failure is still of brittle nature. Remarkable is that the strain to failure from the torsion test is about 2 times higher than the strain to failure obtained from the tension test.

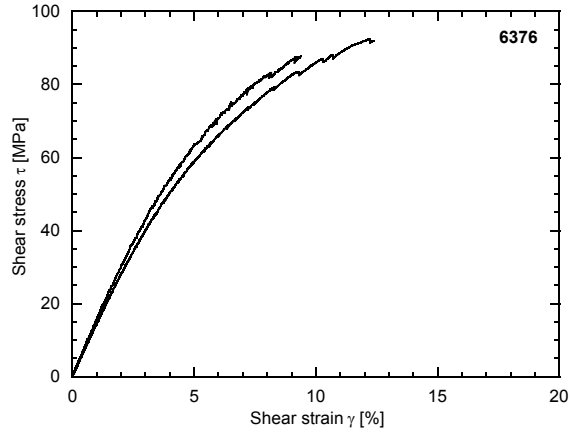

Fig. 3. Stress/strain curves of 6376 obtained from torsional test.

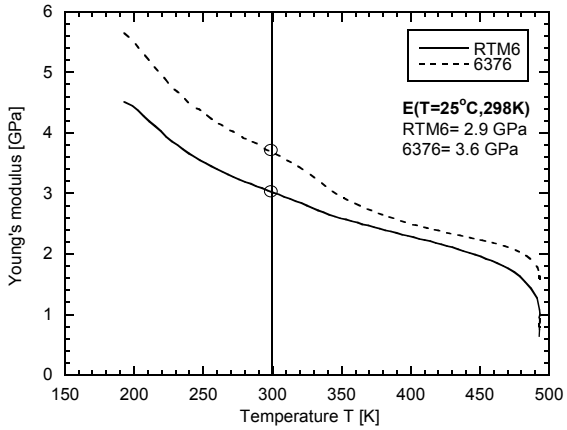

Fig. 4. Temperature dependent Young's modulus of RTM6 and 6376 neat resins.

3.3 DMTA and TMA

Figure 4 shows the temperature dependency of shifted young's modulus of RTM6 and 6373. The Young's modulus of RTM6 decreases with increasing temperature and drops rapidly at 490K (220°C). This dependency is characteristic for an unmodified epoxy resin. 6376 shows almost the same dependency with a small kink between 330K to 350K, which indicates that 6376 is a modified thermoset.

The coefficient of thermal expansion of 6376 obtained from TMA showed a linear temperature dependency. Since the measurement started from 35°C, the CTE's for lower temperatures were extrapolated from the linear dependency. The CTE of RTM6 increases from $54.5\times10^{-6}K^{-1}$ at 25°C to $65.1\times10^{-6}K^{-1}$ at 180°C and for 6376 from $48\times10^{-6}K^{-1}$ at 25°C to $60.3\times10^{-6}K^{-1}$ at 180°C.

2. PARABOLIC FAILURE CRITERION

Yielding and fracture strongly depend on the maximum stress values and their tri-axiality. Therefore, criteria are necessary in order to predict yielding and failure of the matrix under tri-axial stress states. Manjoine [7] gives a good overview about common criteria. In this work, we used the v.Mises criterion for yielding and the parabolic criterion to predict failure of the thermosetting matrix. This criterion is considered to be the most realistic to describe failure behaviour of polymeric materials [3, 8] in which the hydrostatic component of the stress state is taken into account. The parabolic criterion can be expressed in terms of the octahedral stresses σ_0 and τ_0 according to mathematical formulation of Tschoegl [9] as following equation.

$$\tau_0^2 = a_1 - a_2\sigma_0 \tag{2}$$

with the octahedral stresses σ_0

$$\sigma_0 = \frac{\sigma_1 + \sigma_2 + \sigma_3}{3} \tag{3}$$

and τ_0

$$\tau_0 = \frac{\sqrt{(\sigma_1 - \sigma_2)^2 + (\sigma_2 - \sigma_3)^2 + (\sigma_1 - \sigma_3)^2}}{3} \tag{4}$$

The two constants a_1 and a_2 were determined from the fracture stress obtained from the torsion and tension test. Figure 5 shows the parabolic failure surfaces as well as the v.Mises yield surfaces in terms of the octahedral stresses. The failure surface parameter are a_1=3864 and a_2=75.3 for RTM6 and a_1=5692 and a_2=77.4 for 6376. The full dots T and S represent the tensile and shear strength, respectively.

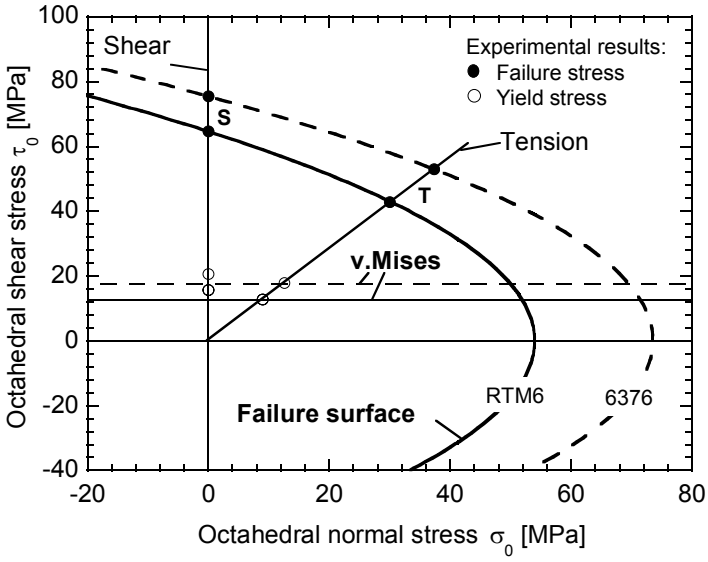

Fig. 5. Parabolic failure surfaces (bold lines) and v.Mises yield surfaces (thin lines) for RTM6 (solid) and 6376 (dashed).

For further work it is more convenient to give the ratio of the present stress state to the failure surface. Therefore we introduce a failure index k.

$$k = \frac{\tau_0}{\tau_{0f}} = \frac{(\sigma_1 - \sigma_2)^2 + (\sigma_2 - \sigma_3)^2 + (\sigma_1 - \sigma_3)^2}{9(a_1 - a_2(\sigma_1 + \sigma_2 + \sigma_3))} \tag{5}$$

k is the octahedral shear stress normalized by the octahedral shear stress given by the failure criterion. A value of k=1 means the material fails.

3. NUMERICAL CALCULATION

The commercial finite element software Marc™ (version 2003) with the pre- and postprocessor Mentat™ was used to carry out the FE- calculations. The models consist of a discrete unit cell of fibres in a hexagonal array in the matrix. The fibre volume fraction was V_f=60%. The finite element model is shown schematically in Fig. 6. The model is made by two-dimensional four node plane strain elements. The boundary conditions are fixed displacement in x-direction for the left edge (A-B) and fixed displacement in y-direction for the nodes at the lower edge (B-C). In the case of the cross-ply laminate, the edge (C-D) was constrained to remain straight after deformation in order to avoid edge effects from the free surface. A load in x-direction was applied after a temperature change from 180°C to 25°C according to the manufacturing temperature. The fibres and the homogeneous area were taken as orthotropic materials. The epoxy matrix was assumed to be isotropic with temperature dependent mechanical properties.

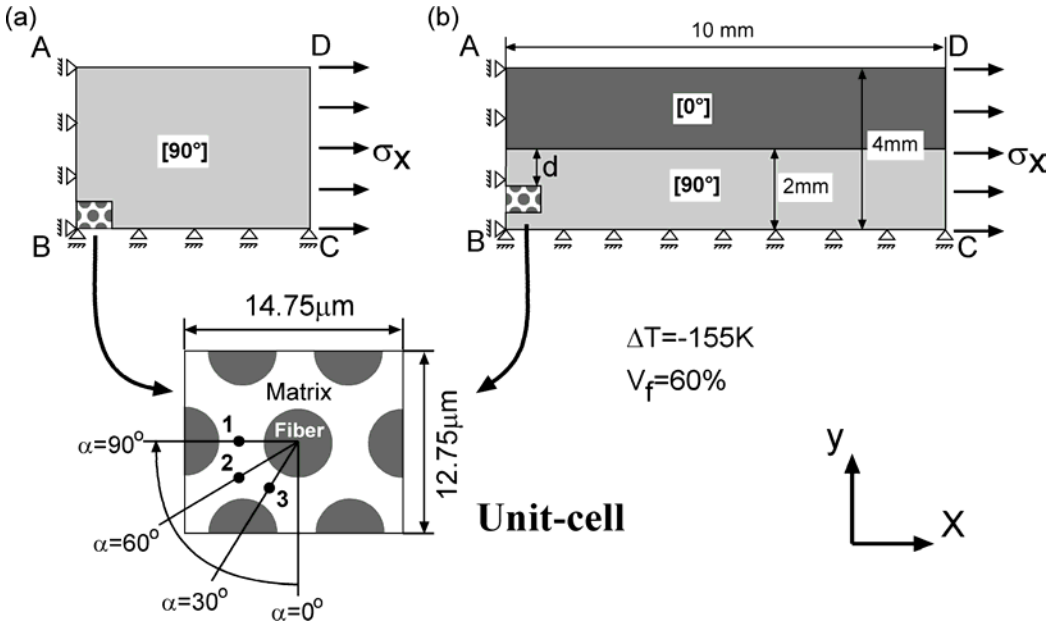

Fig. 6. Schematic illustration of the FE-models for a UD-laminate (a) and a cross-ply laminate (b).

4. RESULTS & DISCUSSION

4.1 Failure initiation in UD- and cross-ply laminates

Figure 7 shows the distribution of the failure index k for CF/RTM6 (a) and for CF/6376 (b), at the moment of failure initiation. Since matrix failure was considered as the governing failure mechanism, the fibres are not displayed for a better clearness. The figures show that initial failure occurs between the fibres where the fibres have their closest interfiber distance. The initiation point is the fibre/matrix interface in the closest location to the neighbouring fibre. In the case of RTM6 the applied load σ_1 at initiation of failure was 37 MPa for CF/RTM6 and 54 MPa for CF/6376, and these values are smaller than the failure stress of the neat resin with σ_f=87.5 MPa (RTM6) and σ_f=102.9 MPa (6376). This difference comes from thermal residual stresses as well as the tri-axial stress state in the composites. In other words the composite is already preloaded in the microscopic level before application of a mechanical load. Since the residual stresses are generated during the cooling process at higher temperatures, where the yield stress is lower than that at room temperature, matrix yielding

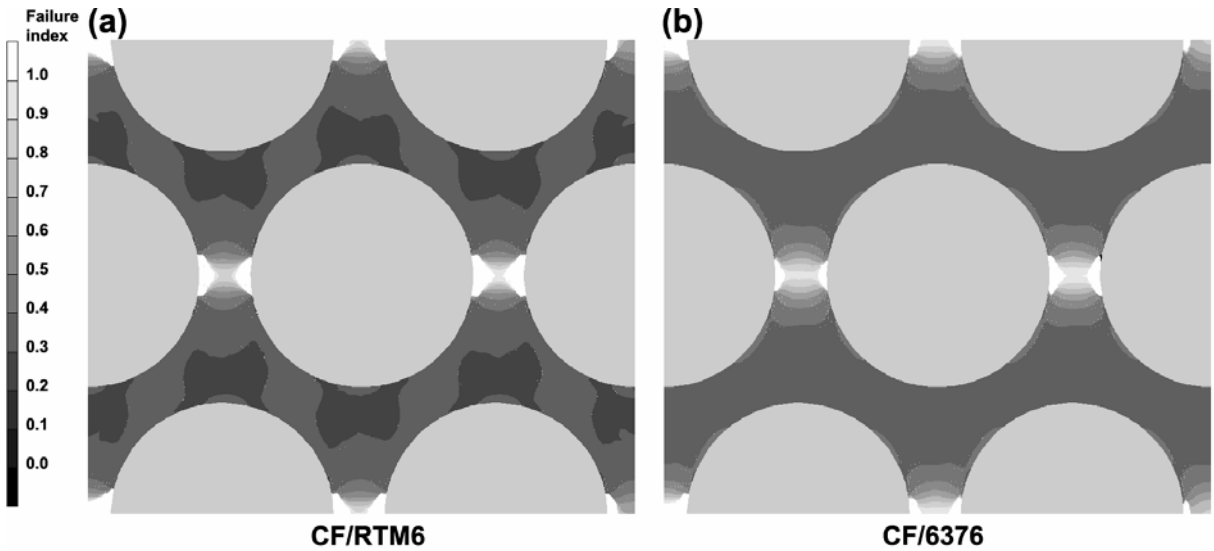

Fig. 7. Pattern of the failure index k for CF/RTM6 (a) and for CF/6376 (b) at failure initiation.

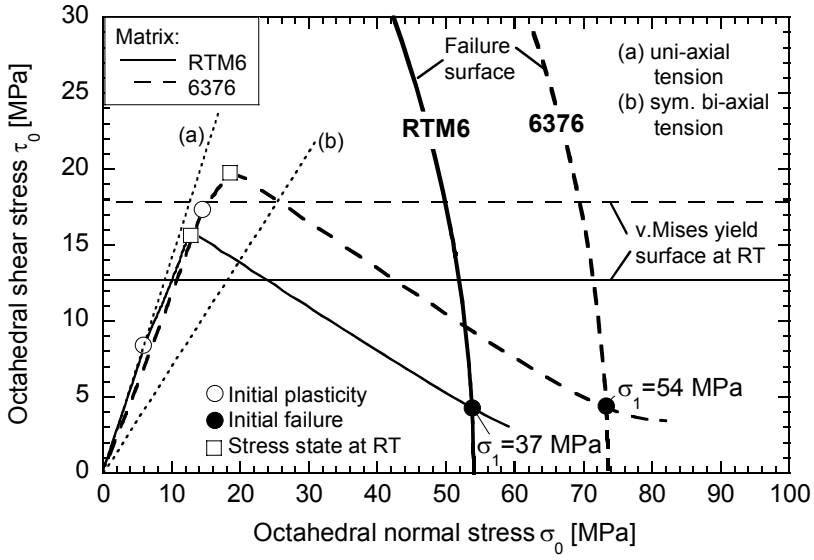

Fig. 8. Formation of microscopic stresses in the 90°-layer of a RTM6 and 6376 UD-laminate during cooling and loading.

will influence the formation of residual stresses. Figure 8 shows the formation of residual stresses at location of first failure in a UD-laminate with RTM6 and 6376 as matrix in terms of octahedral stresses. Furthermore, bold lines show the failure surfaces for RTM6 and 6376. For comparison, dotted lines show uni- and symmetric bi-axial stress states. Symmetric tri-axial or hydrostatic stress states are equivalent with the x-axis. This figure clearly shows that the formation of microscopic stresses during cooling is almost uni-axial tension in a UD-laminate. After cooling to room temperature, the matrix stress states for both composites are within the resin failure surfaces. Therefore, failure during cooling under this cooling and boundary conditions can be excluded. With an applied mechanical load, the octahedral shear stresses decrease, this means the microscopic stress state becomes more tri-axial. Failure occurs at σ_1=37 MPa for CF/RTM6 and σ_1=54 MPa for CF/6376. Interesting is, that the residual stresses in the CF/6376 composite are higher than that in the CF/RTM6 composite, even though the CTE of 6376 is lower than that of RTM6. This is due to the higher Young's modulus of 6376. Then, the lower CTE of 6376 yields lower thermal strains in the CF/6376 composite.

When the composite is subjected to more complex boundary conditions, the microscopic

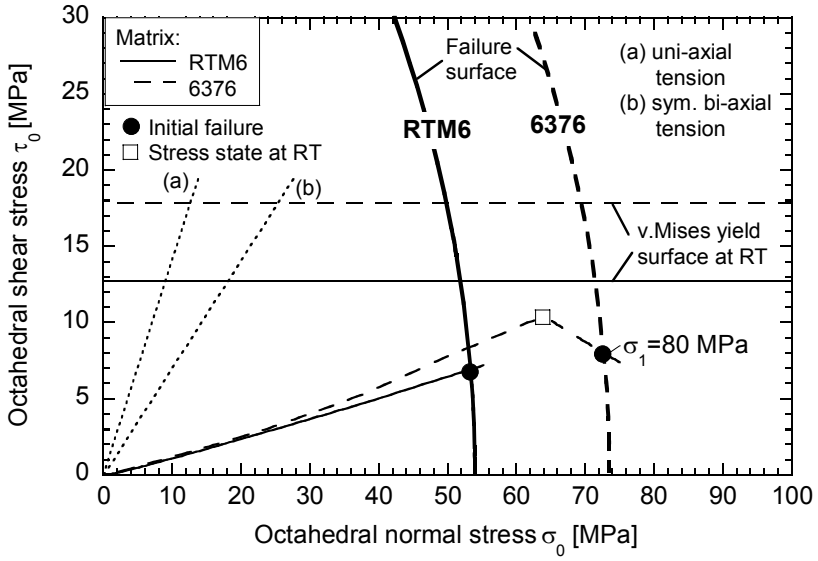

Fig. 9. Formation of microscopic stresses in the 90°-layer of a RTM6 and 6376 cross-ply laminate during cooling and loading.

stress state can be more tri-axial. Thus, the elastic/plastic matrix behaviour also will change. The 0°-layer in a cross-ply laminate causes constrained boundary conditions in the 90°-ply during cooling and loading. With decreasing temperature, the thermal contraction of the 0°-layer is smaller than in the 90°-layer. This causes thermal residual stresses, which are tension in the 90°-layer and compression in the 0°-layer, in addition to those caused by the difference of CTE of fibres and matrix. The microscopic stress formation in the 90°-layer of a cross-ply laminate is shown in Fig. 9. The low τ_o and high σ_o indicate that the stress state is almost tri-axial, as a result of the constraint effect of the 0°-layer. No failure occurs in the CF/6376 cross-ply laminate, whereas in the case of the CF/RTM6 cross-ply laminate, failure occurs already during cooling at a temperature of T=77°C. Independent of the boundary conditions (UD-laminate or cross-ply laminate), transverse failure occurs under tri-axial stress states.

4.2 Influence of matrix plasticity on failure initiation

The stress state at location of initial failure in the cross-ply laminate is always below the resin yield surface as shown in Fig. 9. In the UD-laminate the stress state exceed the yield surface and the matrix starts to behave non-linear (Fig.8). To explain the influence of matrix plasticity on the microscopic stress state, Fig. 10 shows the microscopic equivalent stress formation in CF/RTM6 (bold lines) and CF/6376 (thin lines) UD-composites. The stresses were taken at the fiber/matrix interface in the closest location to the neighboring fiber, where initial failure occurs. The results for linear and non-linear calculations are indicated. The stresses are generated in both composites, with cooling down from manufacturing temperature. The increasing rate in thermal residual stresses is higher than that in yield strength. Matrix yielding occurs during cooling at 98°C for RTM6 and at 53°C for 6376. Solid circles indicate the onset of matrix yielding, where the equivalent stresses exceed the resin yield surfaces. From this point the generation of residual stresses in the non-linear calculation is lower than those in the linear calculation. For both matrices, it can be seen that the non-linear calculation yields lower microscopic equivalent stresses. In our former work we showed that matrix yielding at one position in the matrix causes a stress redistribution,

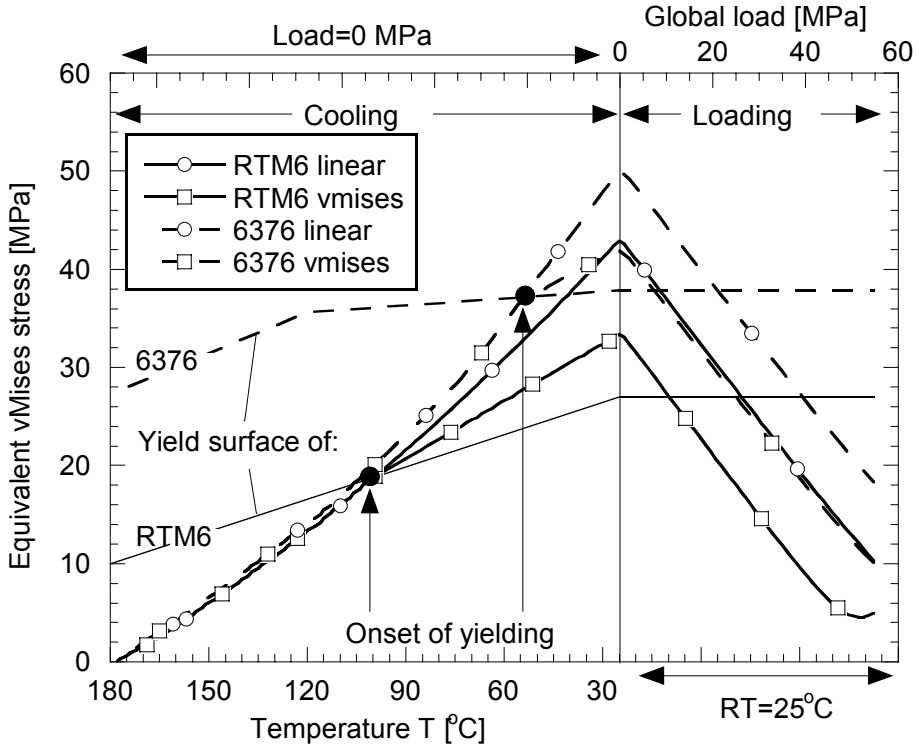

Fig. 10. Formation of equivalent v.Mises stress in CF/RTM6 and CF/6376 UD-laminate for a linear and non-linear matrix behaviour.

which results in a global stress reduction also at positions where the matrix behavior is linear elastic. This means the stress state in the entire matrix will be lower for the non-linear calculation. The maximum global load σ_1 without matrix failure in a UD-laminate is lower for the linear elastic calculation, 34 MPa for CF/RTM6 and 52 MPa for CF/6376 than for the non-linear calculation 37 MPa for CF/RTM6 and 54 MPa for CF/6376.

Fig. 10 shows furthermore that the microscopic stress state caused by mechanical loading results in decreased equivalent v.Mises stresses. In contrast to the lower stresses caused by matrix yielding, the microscopic stress state becomes more tri-axial and not smaller under mechanical loading. Therefore the stress state will fall below the v.Mises yield surface and the material behaves linear elastic resulting in almost brittle matrix failure.

5. SUMMARY

The present work we determined the formation of microscopic stresses under thermal and mechanical loadings. Our non-linear calculations show that microscopic yielding of the polymeric matrix occurs in a UD-laminate during cooling and lead to decrease of residual stresses and increase of maximum macroscopic bearable load for CF-epoxy laminates. However the final matrix failure in a composite is still of brittle nature because the microscopic stress at location is highly tri-axial which suppress matrix yielding.

ACKNOWLEDGEMENTS

This work was supported in the frame of the collaborative program of the German Research Foundation (DFG) and the Japan Society for the Promotion of Science (JSPS).

Grateful thanks to the Ministry of Education, Culture, Sports, Science and Technology for the International Doctoral Program in Engineering at Graduate School of Engineering, Kyoto University.

The authors acknowledge to the Center of Excellence COE for Research and Education on Complex Functional Mechanical Systems for their support.

References

1. **Asp L.E., Berglund L.A. and Talreja R.** "Prediction of matrix-initiated transverse failure in polymer composites", *Compos Sci Technol, **56** (1996), 1089-1097.*
2. **Wang W.X., Takao Y. and Suhara T.** "An approximate solution of stress field in unidirectional composites under tensile und thermal loading", *J Society Mat Sci Japan, **36** (1987), 202-208.*
3. **Fiedler B., Hojo M., Ochiai S., Schulte K. and Ando M.** "Failure behavior of an epoxy matrix under different kinds of static loading", *Compos Sci Technol, **61** (2001), 1615-1624.*
4. **Hull D. and Clyne T.W.** (Editors)An introduction to composite materials. (1996), Cambridge University Press, Cambridge.
5. **Fiedler B., Hojo M., Ochiai S., Schulte K. and Ochi M.** "Finite-element modeling of initial matrix failure in CFRP under static transverse tensile load", *Compos Sci Technol, **61** (2001), 95-105.*
6. **Hobbiebrunken T., Hojo M., Fiedler B., Tanaka M., Ochiai S. and Schulte K.** "Thermomechanical analysis of micromechanical formation of residual stresses initial matrix failure in CFRP", *JSME International Journal Series A, **47** (2004), accepted.*
7. **Manjoine M.J**. Multiaxial stress and fracture. In Fracture. An Advance Treatise. Edited by Libowitz H. 3, (1971), pp 265-309. Academic Press, New York, London.
8. **Fiedler B., Hojo M. and Ochiai S.** "The parabolic failure criterion applied to epoxy resins", *Proceedings of international conference on new challenges in mesomechanics, Aalbourg, Denmark, (2002), 533-539.*
9. **Tschoegl N.W.** "Failure surfaces in principal stress spaces", *J Polymer Sci Part C Polymer Symposia, **32** (1971), 239-267.*